

# P-Glycoprotein Expression by Technetium-99m-MIBI Scintigraphy in Hematologic Malignancy

Lale Kostakoglu, Dicle Guc, Hande Canpinar, Ayse Kars, Eray Alper, Pinar Kiratli, Mutlu Hayran, Ufuk Gunduz and Emin Kansu

Departments of Nuclear Medicine and Medical Oncology, Hacettepe University Medical Faculty, Ankara; Departments of Basic Oncology and Cancer Epidemiology, Hacettepe University Oncology Institute, Ankara; Department of Nuclear Medicine, Uludag University Medical Faculty, Bursa; and Department of Biology, Middle East Technical Universtiy, Ankara, Turkey

Our aim was to ascertain the relationship between the degree of  $^{99m}\text{Tc}$ -MIBI uptake and the level of p-glycoprotein (Pgp) expression determined by flow cytometry and reverse transcription-polymerase chain reaction (RT-PCR) techniques in patients with hematologic malignancy. **Methods:** A total of 21 samples (19 patients) were evaluated. Two patients had repeat studies after therapy. Thirteen samples were studied at the time of initial diagnosis and 8 during relapse after therapy. After MIBI imaging, either bone marrow aspiration or peripheral blood was obtained for flow cytometric and RT-PCR analyses. Flow cytometry was performed using two different antibodies. After the injection of 555 MBq MIBI, whole-body and pelvic spot images were acquired using a dual-head gamma camera. The uptake in the bone marrow was evaluated against the background (adjacent soft tissue) by both qualitative (scoring system) and quantitative (tm/bkg ratios) analyses. **Results:** For flow cytometry, the limit for Pgp overexpression was set at >15% Pgp-positive mononuclear bone marrow or peripheral blood cells. There was an inverse correlation between the levels of Pgp and MIBI imaging using both the qualitative (scoring system) and quantitative (tm/bkg ratios) analyses ( $p = 0.022$ ). Mean values were statistically different between Pgp + and Pgp - groups for both qualitative and quantitative analyses ( $p = 0.009$  and  $0.024$ , respectively). For RT-PCR, there was statistical support toward a difference in the mean values between Pgp + and Pgp - groups by qualitative analysis ( $p = 0.061$ ); however, no statistical difference was found between these two groups by quantitative analysis ( $p = 0.179$ ). **Conclusion:** Based on the strong correlation between the imaging and flow cytometry and a statistical support toward the correlation between the imaging and RT-PCR, MIBI imaging may be used for the in vivo detection of Pgp in patients with hematologic malignancy.

**Key Words:** multidrug resistance; p-glycoprotein; technetium-99m-MIBI; reverse transcription-polymerase chain reaction techniques; flow cytometry

**J Nucl Med 1998; 39:1191-1197**

Despite the introduction of more effective drugs, treatment success has been stunted by chemotherapy failure due to cellular drug resistance, which still remains a major problem in most cancers. Establishment of better designed chemotherapy strategies may further improve survival rates.

Attention has focused lately on the expression of the p-glycoprotein (Pgp)/multidrug-resistance gene (MDR1) gene as an important determinant of responsiveness to therapy and survival in a group of cancers including hematologic malignancies (1-7). As the modulation of the Pgp-mediated multidrug resistance (MDR) phenotype has opened prospects for a better response to therapy, various methods have been developed to

increase the sensitivity and accuracy of detection techniques (3-7). MDR1 gene expression has, thus far, been investigated by using different probes or by studying the increase of MDR1 mRNA or the protein expression of Pgp (8-11). On the other hand, an organotechnetium complex, MIBI, has been reported to be a transport substrate for Pgp (12,13). Although its accumulation rates are driven by negative transmembrane potential, the accumulation of MIBI is reduced in cells expressing the MDR phenotype because of the energy-dependent Pgp efflux pump, which causes decreased accumulation of its substrates (12-15). Previous studies have shown an inverse relationship between Pgp levels and the magnitude of MIBI uptake (16-19). There still exists a need for the functional imaging data to be correlated with other objective techniques performed at the molecular level to verify MIBI findings.

Because accurate detection of Pgp/MDR1 gene has important clinical implications and verification of antigenic expression at the molecular level is considered a gold standard, in this study we investigated the diagnostic potential of MIBI for determining Pgp compared to flow cytometry and reverse transcription-polymerase chain reaction (RT-PCR) to demonstrate a correlation between imaging and molecular studies in patients with hematologic malignancy.

## MATERIALS AND METHODS

### Patients

A total of 21 specimens were included in our study from 19 patients (age range 30-70 yr; mean age  $47.3 \pm 13.8$  yr). Twelve patients had acute myelocytic leukemia (AML) and 7 had acute lymphoblastic leukemia. Eleven patients were evaluated before chemotherapy. Eight of 19 patients had been previously treated with various chemotherapy regimens consisting of doxorubicin, mitomycin, vincristine, methotrexate, mitoxantrone, cytosine arabinoside and idarubicin. Bone marrow aspiration or peripheral blood were obtained for flow cytometric and RT-PCR analyses in all patients 1-3 days before imaging studies. In 2 of 19 patients, all studies were repeated during relapse 3 mo after initial therapy, and a total of 21 samples were obtained. Data were available for both flow cytometry and RT-PCR on 10 samples, and on 11 samples either flow cytometric analysis (7 samples) or RT-PCR (4 samples) was performed. To increase the specificity of the flow cytometric analyses, two different antibodies were used in 15 samples, one developed against the internal (JSB-1) and one against the external epitope (UIC2) of the Pgp antigen. These 15 samples included those 7 on which RT-PCR could not be performed.

### Imaging

Images were obtained 20-30 min postinjection of 740 MBq  $^{99m}\text{Tc}$ -MIBI. A dual-head ADAC Genesys camera with a LEHR collimator interfaced with an ADAC 3300 computer was used for

Received Jun. 11, 1997; revision accepted Oct. 13, 1997.

For correspondence or reprints contact: Lale Kostakoglu, MD, New York Hospital-Cornell Medical Center, Nuclear Medicine Division, 525 East 68th Street, Starr Bldg. 221, New York, NY 10021.

**TABLE 1**  
Qualitative Scoring Results of MIBI Imaging

Patient no.	Humerus	SJ	Sternum	AIC	TM	SI	Femur	Mean
1	1	1	1	2	2	2	1-2	1.50 r
2	2	2-3	3	3	3	2	3	2.62
3	2	3	2	3	3	3	3	2.71 r
4	2	3	2	3	2-3	3	3	2.62 r
5	1	3	3	2-3	3	3	3	2.71
6	1	2	1-2	1-2	2	2	2	1.67
7	2	3	2-3	2	2-3	3	2-3	2.50
8	2	3	2	2-3	2	2-3	2	2.33 r
9	1	2	1-2	1-2	3	2	2-3	1.90
10	1	1	2	2-3	2	2	1	1.75
11	2	2-3	2-3	3	3	3	3	2.67
12	2	3	3	3	3	3	2	2.71
13	1	2	2	2-3	3	3	1-2	2.11
14	1	2	1-2	2-3	2	2	2	1.88 r
15	2	2-3	2	3	3	3	2-3	2.55
16	1-2	2	2	2	2	3	2-3	2.11
17	1	1-2	1-2	3	2	2-3	2	1.90 r
18	1-2	2	2	2	2	2-3	2	2.00 r
19	1	2	1	3	2-3	2-3	1	2.00 r
20	2	3	2-3	3	3	3	3	2.75
21	2	2-3	2	3	3	3	3	2.62

SJ = shoulder joint; AIC = anterior iliac crest; TM = trochanter major; SI = sacroiliac joints; r = patients presented with relapse.

**TABLE 2**  
Quantitative Scoring Results of MIBI Imaging

Patient no.	Humerus	SJ	Sternum	AIC	TM	SI	Femur	Mean
1	0.45	0.55	0.84	1.26	1.20	1.30	1.26	0.98 r
2	0.80	1.10	1.38	1.93	1.82	1.65	1.61	1.46
3	0.90	1.00	1.25	1.85	1.49	2.10	1.20	1.38 r
4	0.80	1.00	1.20	1.66	1.67	2.10	1.30	1.38 r
5	1.00	1.37	1.53	1.63	1.55	2.10	1.20	1.48
6	0.50	0.85	0.90	1.00	1.30	1.45	1.12	1.01
7	1.00	1.30	1.20	1.20	1.20	1.40	1.00	1.20
8	1.00	1.00	1.00	1.45	1.3	1.55	1.20	1.21 r
9	0.60	0.85	1.00	1.20	1.34	1.35	1.25	1.10
10	0.45	0.57	1.16	1.43	1.20	1.00	0.85	0.95
11	0.80	0.90	1.42	1.60	1.85	1.75	1.20	1.35
12	1.00	1.60	1.45	1.95	1.82	2.05	1.30	1.59
13	0.70	0.81	1.00	1.40	1.37	1.85	1.00	1.16
14	0.70	0.80	0.90	1.20	1.20	1.30	1.00	1.01 r
15	0.70	0.85	1.00	2.10	2.00	1.70	1.35	1.39
16	0.69	1.00	1.11	1.30	1.20	1.90	1.16	1.19
17	0.80	0.90	1.00	1.30	1.20	1.30	1.10	1.08 r
18	0.65	0.81	1.00	1.48	1.30	1.55	1.10	1.15 r
19	1.00	0.96	1.00	1.57	1.40	1.51	1.00	1.20 r
20	1.50	1.60	1.35	1.63	1.95	1.98	1.70	1.67
21	1.30	1.20	1.20	1.65	1.60	1.71	1.30	1.42

SJ = shoulder joint; AIC = anterior iliac crest; TM = trochanter major; SI = sacroiliac joints; r = patients presented with relapse.

image acquisition. Whole-body and planar spot images of the pelvis were acquired. The uptake ratios were taken in the regions of interests drawn over relevant areas containing tumor (bone marrow) and the contralateral site.

MIBI scans were interpreted by two nuclear medicine physicians blinded to the patients' clinical information, flow cytometry and RT-PCR findings.

Uptake of MIBI in the target organ (bone marrow) was evaluated against the uptake in the reference organ (reference organ uptake was defined as the adjacent soft tissue uptake). This evaluation was performed using a qualitative scoring system (Table 1) with the following criteria: (a) bone marrow uptake < soft tissue uptake = 1; (b) bone marrow uptake = soft tissue uptake = 2; and (c) bone marrow uptake > soft tissue uptake = 3.

This evaluation was also performed using a quantitative system with the determination of tumor-to-background (tm/bkg) ratios (Table 2). Both the qualitative and quantitative analyses were performed in the bone marrow in areas that included the proximal humerus, shoulder joints, sternum, anterior iliac crests, trochanter majors, sacroiliac joints and proximal femurs. Mean values were determined for both the qualitative and quantitative analyses (Tables 1 and 2). For symmetric organs, a mean value was derived for the values obtained bilaterally. To avoid false-positive results that could originate from the overlapping physiologic uptake in the heart, kidneys and bowels, the vertebral column was not included in the analyses.

### Flow Cytometry

The leukemic blast cells were separated from heparinized peripheral blood or bone marrow on ficoll hypaque by density gradient. Pgp expression in blast cells was determined by indirect immunofluorescence using JSB-1 (Boehringer Mannheim, Mannheim, Germany) and UIC2 (Dr. Carlos Cardon-Cardo, Memorial Sloan Kettering Cancer Center, NY) antibodies. As JSB-1 has a specificity for an internal epitope, for fixation the blast cells were resuspended in 70% cold methanol and incubated for 5 min at -20°C to permeabilize the cell membrane. The cells were then

washed twice and resuspended in PBS + 0.05%NaN<sub>3</sub>. Blast cells, 1 × 10<sup>6</sup>, were then incubated with the antibodies, JSB-1 and UIC2, prepared at a final concentration of 10 μg/ml for 60 min at 4°C and then washed and incubated with fluorescein isothiocyanate-conjugated sheep antimouse IgG serum (Dako, Versailles, France) for 30 min at 4°C. The cells were then washed and analyzed with a flow cytometer, EPICS 541, (Coulter, Luton, UK). An irrelevant, isotype-matched mouse IgG (Sigma Chemical Co., St. Louis, MO) was used as a negative control. The blast cell population was gated using scatter parameters. Staining was considered positive when more than 15% of the cells were stained.

### Total RNA Extraction and Detecting Gene Expression by Reverse Transcription-Polymerase Chain Reaction

The RNAzol method was used to isolate cellular RNA (20). Complementary DNA (cDNA) was synthesized with 1 μg of total cellular RNA, 100 ng of random primers (MWG-Biotech, Münchenstein, Germany) and 125U of MO MULV reverse transcriptase (Superscript Rnase H-Reverse transcriptase; BRL) at 37°C for 60 min. PCR was performed with cDNA aliquots equivalent to 1 μg of RNA, 2 μmol/liter of MDR1 specific primers and 1 unit of thermus aquaticus DNA polymerase (MBI-Fermentas, Vilnius, Lithuania) in a final volume of 20 μl. PCR was performed in a thermal cycler, PTC-100, (MJ Research Inc., Watertown, MA) for 35 cycles. Each cycle included 1 min of denaturation at 94°C, 1 min of primer annealing at 57°C and 1 min of DNA extension at 72°C. PCR products (10 μl/reaction) were analyzed by electrophoresis on 2% agarose gel. MDR1-specific sequences were amplified using the following primers: sense strand; 5'CCCAT-CATTGCAATAGCAGG3', and antisense strand; 5'GT-TCAAACCTTCTG-CTCCTGA3' (MWG-Biotech, Münchenstein, Germany). These primers generate a 167-kb PCR product.

### Statistical Analysis

The correlation between flow cytometry and MIBI results (qualitative and quantitative analyses) and between MIBI results from the two different antibodies were analyzed by Spearman's rank correlation coefficient. Kappa statistics were used to define

**TABLE 3**  
Correlation of MIBI Parameters with Flow Cytometry and Reverse Transcription-Polymerase Chain Reaction (RT-PCR) Results

Dx	MIBI scintigraphy		Molecular studies		
	Qualitative (scoring)	Quantitative (tm/bkg)	FC		RT-PCR
			MAb1	MAb2	
1 AML*	2.00	1.08	83%	np	+ r
2 AML	1.90	1.10	74%	76%	+
3 AML	2.00	1.20	43%	26%	np r
4 ALL	1.75	0.95	32%	34%	np
5 AML	2.62	1.42	27%	46%	+
6 ALL	1.67	1.01	26%	56%	np
7 AML	2.11	1.16	24%	25%	np
8 ALL*	2.11	1.19	16%	10%	+
9 ALL	1.50	0.98	np	np	+ r
10 AML	1.88	1.01	np	np	+ r
11 AML	2.62	1.46	13%	np	-
12 AML	2.71	1.48	12%	10%	-
13 ALL*	1.90	1.15	10%	12%	np r
14 AML	2.75	1.67	9.0%	8.0%	+
15 ALL	2.71	1.38	8.3%	7.0%	- r
16 ALL	2.33	1.21	2.0%	3.0%	- r
17 ALL	2.50	1.20	-	-	np
18 AML	2.67	1.35	-	-	np
19 AML*	2.55	1.39	4.1%	4.3%	-
20 AML	2.62	1.38	np	np	- r
21 AML	2.71	1.59	np	np	-

\*Samples 1 and 19 and 8 and 13 represent the same patient studied after therapy and before therapy, respectively.

ALL = acute lymphocytic leukemia; AML = acute myelogenous leukemia; Dx = diagnosis; FC = flow cytometry; MAb 1 = antibody 1 - JSB-1; MAb 2 = antibody 2 - UIC2; tm/bkg = tumor-to-background ratio; np = not performed; r = patients presented with relapse.

the concordance between flow cytometry and RT-PCR results. The difference in MIBI values between Pgp + and Pgp - patients who were grouped using the flow cytometry results (Pgp considered positive when either antibody revealed a test result of >15%) was analyzed by the Mann-Whitney test. The cutoff values of 2.33 and 1.20 yielding the highest predictive value were used for determining sensitivity and specificity of MIBI results with respect to the threshold of 15% for Pgp positivity.

## RESULTS

### Flow Cytometry

In all patients, the bone marrow was infiltrated with blast cells with levels ranging from 90%–95%. Flow cytometric data were available in 17 of 21 samples. In 15 samples, flow cytometry was performed using two antibodies, one developed against the internal (JSB-1) and one against the external epitope (UIC2) of the Pgp antigen (Table 3). According to our results obtained in healthy volunteers, the limit for Pgp overexpression was set at 15% Pgp-positive mononuclear bone marrow cells and peripheral blood cells. Eight samples were positive for Pgp with the levels ranging from 16% to 83%, whereas 9 were negative with the levels ranging from 2% to 13% (Table 3). In one of those two patients on whom the studies were repeated during relapse following initial therapy, Pgp converted to positive after therapy (Table 3, Samples 19 and 1, pretherapy and post-therapy, respectively, Fig. 1).

There was good agreement between the two antibodies for determining the Pgp levels in numeric values ( $r = 0.952$ ;  $p < 0.0001$ ; Spearman's rank correlation coefficient) and, with the threshold set at 15% for Pgp positivity, there was also agree-

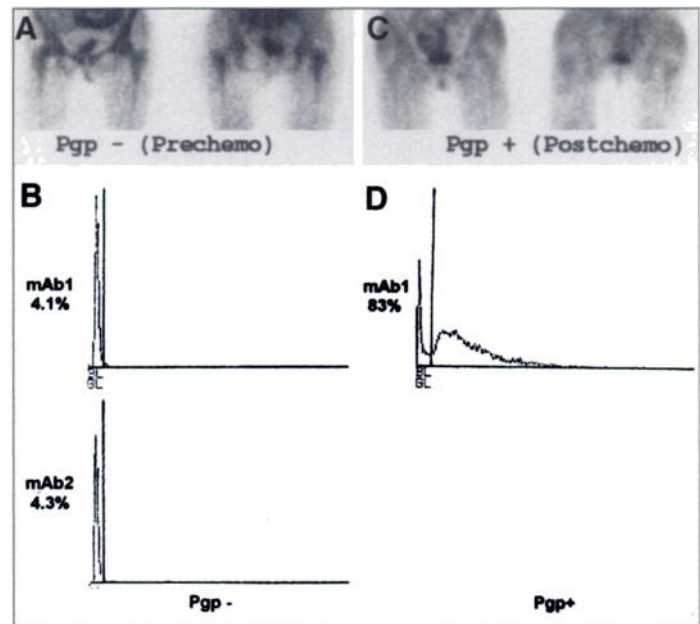


**FIGURE 1.** (A) A 35-yr-old woman who was diagnosed with acute myelocytic leukemia. Pelvic spot views of MIBI imaging demonstrate prominent uptake in pelvic bone marrow consistent with absence of Pgp expression. (B) Pelvic spot views obtained after therapy reveal faint uptake in pelvic bone marrow, which suggests Pgp overexpression induced by cytotoxic drug therapy. (C) Flow cytometric analysis performed before therapy reveals no Pgp overexpression, with levels of 4.1% and 4.3% for MAb1 and MAb2, respectively. (D) Flow cytometric analysis performed after therapy reveals Pgp overexpression, with level of 83% for MAb1. This particular sample could not be studied with MAb2.

ment between the two antibodies ( $r = 86.5\%$ ;  $s.e. = 12.9$ ; Kappa statistics) (Table 3).

### Reverse Transcription-Polymerase Chain Reaction

RT-PCR data were available in 14 samples. Seven samples were positive and 7 were negative for Pgp presence. Both flow cytometry and RT-PCR were performed in 10 samples. When the results of flow cytometry were correlated with those of RT-PCR, the concordance between these two techniques was 80% ( $s.e. = 18.6$ ; Kappa statistics) with Pgp considered positive when either antibody revealed a test result of  $\geq 15\%$ . There was agreement between 9 samples, whereas disagreement was present in 1 sample. In this particular sample, RT-PCR was positive for Pgp when flow cytometry was negative using both antibodies (9% and 8%) (Table 3, Sample 14). The quantitative analyses for RT-PCR was not performed.

### Correlating MIBI Results with Flow Cytometry

There was a statistically significant inverse relationship between the levels of Pgp and both qualitative ( $p = 0.013$ ;  $r = 0.58$ ; Spearman's rank correlation coefficient) and quantitative ( $p = 0.022$ ;  $r = 0.55$ ; Spearman's rank correlation coefficient) results of MIBI imaging (Figs. 2 and 3). The results of the analyses using Mann-Whitney test are as follows.

**Mean Values for Qualitative Analyses.** In Pgp-positive patients, the mean value was  $2.02 \pm 0.29$  (median: 2.00) (Fig. 4A and B), and in Pgp-negative patients the mean value was  $2.53 \pm 0.27$  (median: 2.62) (Fig. 4C and D). There was a statistical difference between these two groups. ( $p = 0.009$ , range: 1.67–2.75) (Figs. 2 and 3).

**Mean Values for Quantitative (Tumor-to-Background Ratios) Analyses.** In Pgp-positive patients, the mean value was  $1.14 \pm 0.14$  (median: 1.13) (Fig. 4A and B) and in Pgp-negative patients the mean value was  $1.33 \pm 0.17$  (median: 1.35) (Fig.

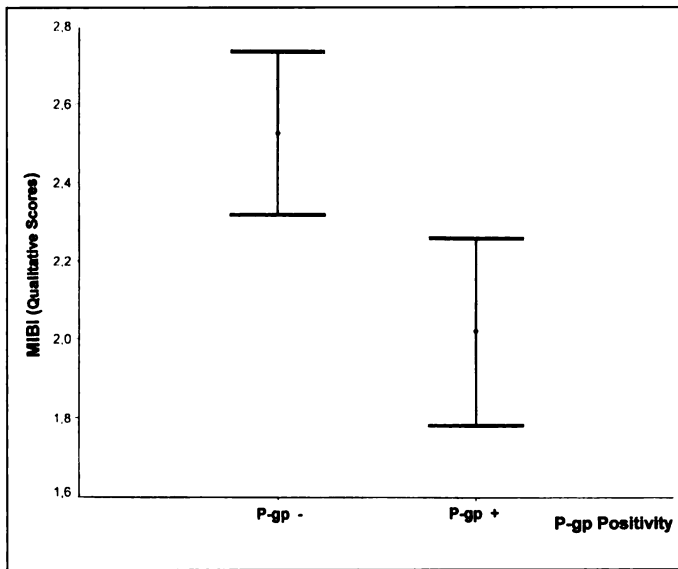


**FIGURE 2.** Distribution of qualitative scores of MIBI imaging in relation to the presence of Pgp expression detected by flow cytometry. Limit for Pgp overexpression was set at  $\geq 15\%$  Pgp-positive mononuclear bone marrow cells or peripheral blood cells. There was inverse correlation between qualitative scores and levels of Pgp expression ( $p = 0.013$ ;  $r = 0.58$ ).

4C and D). There was a statistical difference between these two groups. ( $p = 0.024$ , range: 0.95–1.67) (Figs. 2 and 3).

Sensitivities and specificities of MIBI imaging for detecting Pgp are shown in Table 4. The cutoff values of 2.33 and 1.20 yielding the highest predictive value were used for sensitivity and specificity analyses of MIBI results. There were two patients whose MIBI results contrasted with the cutoff values set for Pgp presence (Table 3, Patient 5 and Patient 13). In one of these patients, although MIBI results indicated no Pgp presence with mean values above the threshold for Pgp presence (qualitative: 2.62 versus 2.33 and quantitative: 1.42 versus 1.20), flow cytometry revealed high levels of Pgp expression using both antibodies (27% and 47%). RT-PCR was in agreement with flow cytometry. In the other patient, MIBI results were consistent with overexpression of Pgp with mean values obtained below the threshold for Pgp presence (qualitative: 1.90 versus 2.33 and quantitative: 1.15 versus 1.20). However, flow

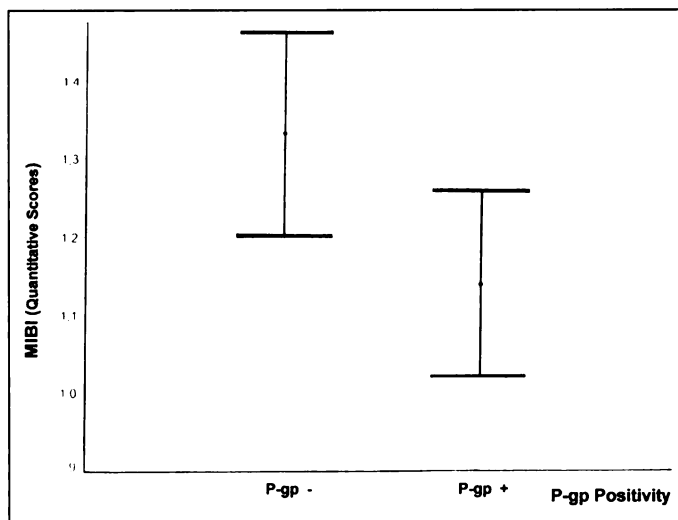


**FIGURE 3.** Distribution of quantitative (tm/bkg) results of MIBI imaging in relation to the presence of Pgp expression detected by flow cytometry. Limit for Pgp overexpression was set at  $\geq 15\%$  Pgp-positive mononuclear bone marrow cells or peripheral blood cells. There was inverse correlation between quantitative results and levels of Pgp expression ( $p = 0.022$ ;  $r = 0.55$ ).

cytometry revealed low levels of Pgp expression (10% and 12%) that are considered to be present in the normal population. In this particular patient, RT-PCR could not be performed.

### Correlation of MIBI Results with Reverse Transcription-Polymerase Chain Reaction

**Mean Values for Qualitative Analyses.** In Pgp-positive patients, the mean value was  $2.13 \pm 0.36$  (median: 2.00) (Figs. 4A and 5) and in Pgp-negative patients the mean value was  $2.59 \pm 0.16$  (median: 2.61) (Figs. 4C and 5). There was statistical support toward a difference between these two groups. ( $p = 0.061$ , range: 1.67–2.75).

**Mean Values for Quantitative (Tumor-to-Background Ratios) Analyses.** In Pgp-positive patients, the mean value was  $1.17 \pm 0.15$  (median: 1.16) (Figs. 4A and 5) and in Pgp-negative patients the mean value was  $1.37 \pm 0.17$  (median: 1.36) (Figs. 4C and 5). A statistical difference could not be found between these two groups ( $p = 0.179$ , range: 0.95–1.67); however, the number of samples was not adequate to arrive at a firm conclusion.

The sensitivity and specificity were 57% and 85% for quantitative and 71% and 100% for qualitative analyses of MIBI imaging (Table 4).

### DISCUSSION

Multiple independent studies have demonstrated that a high level of Pgp expression is associated with a poor response to therapy in patients with acute leukemia or myelodysplastic syndromes (21–23). Further analysis of leukemia specimens has also shown a relationship between Pgp/MDR1 expression and treatment outcome in AML (9,11). As prospective identification of patients with MDR could lead to therapeutic strategies to circumvent or overcome it, such as modulation by various inhibitors or use of chemotherapeutics not involved in the MDR phenotype, multiple detection assays have been developed for accurate characterization of Pgp (24,25). No single detection technique provides specific information on the presence of the Pgp/MDR1 gene, and methods for determining MDR1 expression often yield discordant results. Therefore, the use of at least two methods for evaluating Pgp/MDR1 gene expression is advisable (10,22). RT-PCR is usually recommended because of its relative simplicity and high specificity; however, this technique should be supplemented by immunohistochemistry or flow cytometry to confirm expression of the protein in case there is any blockage in protein synthesis. In our study, we used two techniques and also used two different anti-Pgp antibodies that recognize different epitopes to diminish the possibility of obtaining conflicting results and to improve the reliability of the detection technique.

Because of its recognition as a transport substrate by Pgp, previous studies have indicated a potential use for MIBI for the in vivo identification of the multidrug resistant phenotype in patients with solid tumors (16–19). In line with these studies, the most important finding in our study is the inverse relationship between the Pgp levels detected by flow cytometry and the results of both the qualitative and quantitative (tm/bkg ratios) analyses of MIBI imaging (Figs. 1 and 2). The difference in both qualitative and quantitative values between the Pgp + and Pgp - groups was statistically significant ( $p = 0.009$  and  $0.024$ , respectively). However, there were also contrasting findings in our data. In one patient, MIBI results indicated no Pgp expression while flow cytometry detected high levels of Pgp expression, which was supported by the RT-PCR results. We have to emphasize that imaging findings may not solely be related to the presence of the protein but also to its functional capacity.

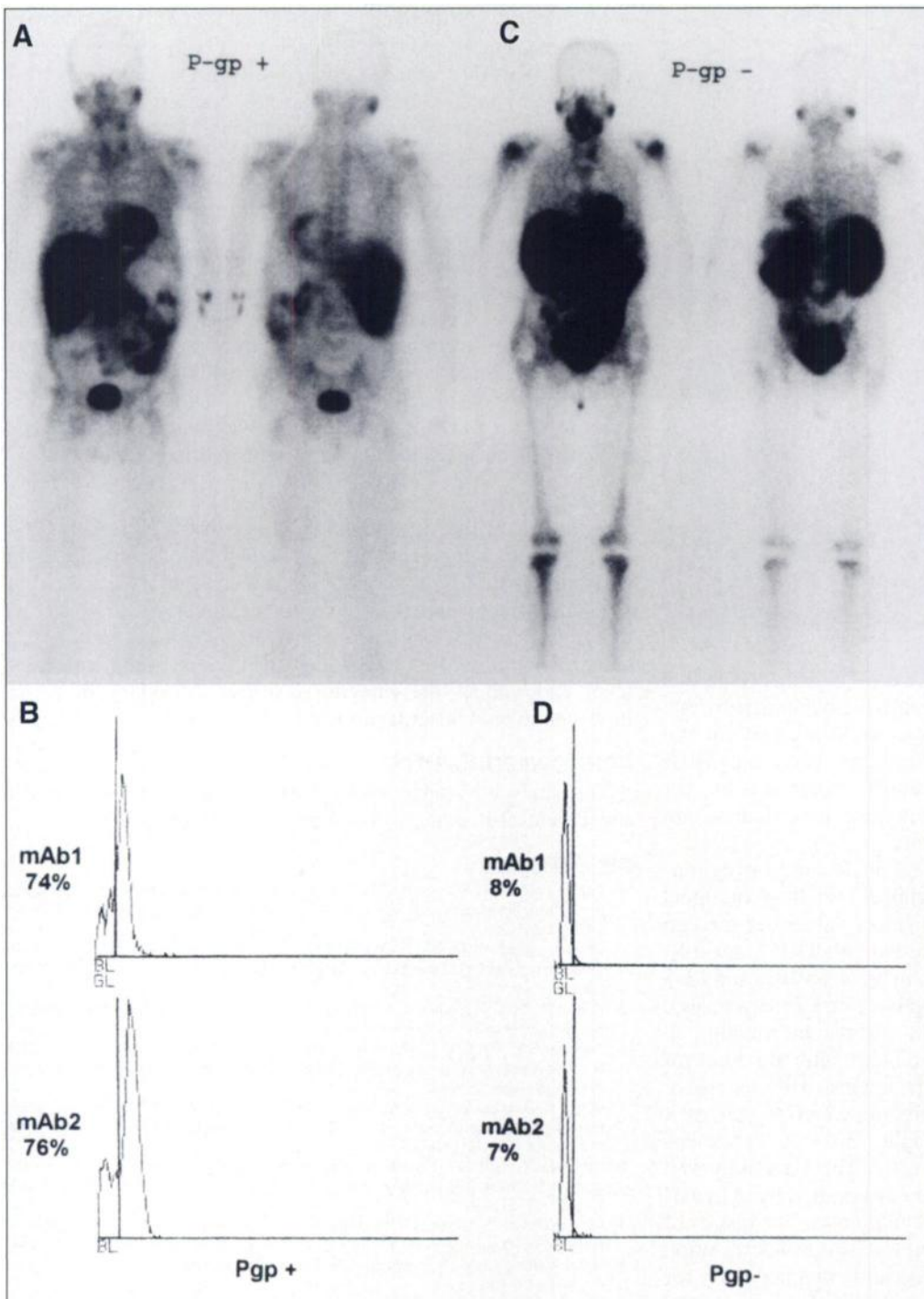


**FIGURE 4.** (A) A 54-yr-old man who was diagnosed with acute myelocytic leukemia (AML). Anterior whole-body views demonstrate only faint uptake of MIBI in bone marrow of shoulder joints, pelvis and proximal femurs. In remainder of body, no appreciable uptake is noted in bone marrow (qualitative: 1.90; quantitative: 1.10). (B) Flow cytometric analysis performed with two antibodies reveals Pgp overexpression, with levels of 74% and 76% for MAb1 and MAb2, respectively. (C) A 44-yr-old woman who was diagnosed with AML. Anterior whole-body views demonstrate prominent bone marrow uptake of MIBI throughout body. (qualitative: 2.71; quantitative: 1.38). (D) Flow cytometric analysis performed with two antibodies does not reveal Pgp overexpression, with levels of 8% and 5% for MAb1 and MAb2, respectively.

Suboptimal functional capacity of the Pgp efflux pump resulting from low levels of the ATP contents of cells could generate conflicting results (3,6,26). Alternatively, the lack of correlation between Pgp expression and function in hematologic malignancies could emerge from distinct differentiation phenotypes. It has been advocated that immunological detection of Pgp should be complemented by functional assays investigating Rhodamine 123 (Rh 123) efflux kinetics that could allow the distinction between typical and atypical MDR phenotypes (26,27). In Bailly et al. (28), when the kinetic profile of Rh 123 release was investigated in AML cells, it was observed that mature phenotypes presented no Rh 123 efflux capacity although they expressed higher Pgp levels, whereas immature cell lines displayed significant Pgp activity.

Although imaging at an earlier period might reflect blood-pool activity, the accumulation of solute molecules in solid and

hematologic tumors varies greatly due to differences in the transport parameters associated with either type of malignancy (29). Once a molecule is injected into the blood stream, the transport process to the hematologic neoplasms, because of their intravascular nature and the lack of transport barriers such as microvascular wall, interstitial space and parenchyma that constitute a resistance to transport molecules to solid tumors, is expected to be faster than to solid tumors. Additionally, high interstitial pressure and low microvascular pressure may retard extravasation of molecules to the tumor parenchyma in solid tumors (29). In our study, imaging patients with hematologic malignancies at 20–30 min should reflect the equilibrium phase affected by the level of Pgp expression.

In one of our patients, when MIBI results were consistent with Pgp expression, with respect to the cutoff values set for Pgp presence, flow cytometry showed only low expression

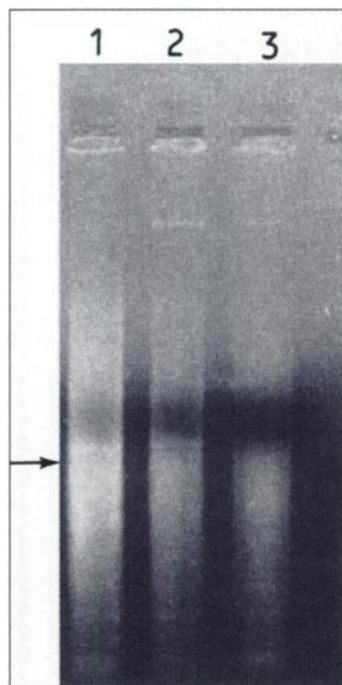


**FIGURE 5.** A 2% agarose gel electrophoresis of MDR1-specific polymerase chain reaction products from patients with acute myelocytic leukemia (Lanes 1, 2 and 3). Lane 1 corresponds to patient described in Figure 4A; Lane 2 corresponds to another patient whose images are not presented here and demonstrates specific product band for MDR1 gene (arrow) (167kb), whereas Lane 3 corresponding to patient described in Figure 4B does not reveal any band representing presence of MDR1 gene.

levels, which were considered negative for Pgp presence. In this patient, poor penetration of the tracer into the bone marrow due to relatively low levels of blood flow could account for the discrepancy between the levels of Pgp expression and MIBI imaging. On the other hand, the cutoff values set for the presence of Pgp should not be relied on until these findings are confirmed on larger number of patients.

There were two samples of which RT-PCR and flow cytometry results were discordant considering RT-PCR as the most sensitive technique regardless of the cutoff values set for Pgp positivity for flow cytometry (Table 3, Patients 11, 12, and 14). In these samples with Pgp levels varying between 10% and 13% on flow cytometry, RT-PCR was negative for Pgp expression. Flow cytometry may fail to provide optimal information in some situations including those specimens with mixtures of normal and malignant cells and specimens with extensive background staining. Therefore, this finding could be consistent with false-positive flow results brought about by specimens with extensive background staining (30). The sensitivity and specificity of certain techniques are always limited by unavoidable parameters such as skill of the technologists. The results of previous studies have suggested a need for clear standardization of the methods for detecting Pgp by revealing that positivity for Pgp depends on various factors including the specificity of the monoclonal antibodies, techniques used and preservation of the samples (5,31).

**TABLE 4**  
Statistical Analyses of MIBI Scintigraphy in Detection of P-Glycoprotein

	Sensitivity	Specificity	PPV	NPV
Flow cytometry				
Qualitative	87.5	89.0	89.0	87.5
Quantitative	75.0	78.0	78.0	75.0
Reverse transcription-polymerase chain reaction				
Qualitative	57.0	85.0	85.0	57.0
Quantitative	71.0	100.0	100.0	71.0

PPV = positive predictive value; NPV = negative predictive value.

In one of our patients, although RT-PCR was positive, protein expression could not be detected by flow cytometry (9% and 8%). This discrepancy between mRNA and protein expression may be related to one of the post-transcriptional control mechanisms such as negative translational control (32) or by the regulation of initiation factor phosphorylation in response to a variety of situations (33). False-positive PCR or false-negative flow cytometry results should also be taken into consideration.

There was statistical support toward a difference in the mean values between Pgp + and - groups for qualitative analysis ( $p = 0.061$ ); however, no statistical difference was found between these two groups for quantitative analysis ( $p = 0.179$ ). This finding could be attributed to the relatively small number of patients we studied. On the other hand, similar factors mentioned for the discrepancies obtained between mRNA and protein expression may also be responsible for this finding.

## CONCLUSION

Although further investigation is necessary to confirm our findings with a larger number of patients, functional imaging performed with MIBI can noninvasively identify MDR phenotype in patients with hematologic malignancy. However, as discrepancies exist between molecular and imaging studies, a combination of current techniques, ideally one at the molecular level and one at the imaging level, is necessary to avoid false-positive or false-negative results.

## ACKNOWLEDGMENTS

This study was supported by Turkish Foundation of Scientific and Technical Research Grant Number SBAG-AYD-82.

## REFERENCES

1. Fojo AT, Ueda K, Slamon DJ, Poplack DG, Gottesman MM, Pastan I. Expression of a multidrug-resistance gene in human tumors and tissues. *Proc Natl Acad Sci USA* 1987;84:265-269.
2. Gros P, Talbot F, Tang-Wai D, Bibi E, Kaback HR. Lipophilic cations: a group of model substrates for the multidrug-resistance transporter. *Biochemistry* 1992;31:1992-1998.
3. Kessel D, Beck WT, Kukuruga D, Schulz V. Characterization of multidrug resistance by fluorescent dyes. *Cancer Res* 1991;51:4665-4670.
4. Noonan KE, Beck WT, Holzmayer TA, et al. Quantitative analysis of MDR1 (multidrug resistance) gene expression in human tumors by polymerase chain reaction. *Proc Natl Acad Sci USA* 1990;87:7160-7164.
5. Longo R, Bensi L, Vecchi A, Messora C, Sacchi S. P-glycoprotein expression in acute myeloblastic leukemia analyzed by immunocytochemistry and flow cytometry. *Leuk Lymphoma* 1995;17:121-125.
6. Ludescher C, Hilbe W, Eisterer W, et al. Activity of p-glycoprotein in B-cell chronic lymphocytic leukemia determined by a flow cytometric assay. *J Natl Cancer Inst* 1993;85:1751-1758.
7. van der Heyden S, Gheuens E, DeBruijn E, Van Oosterom A, Maes R. P-glycoprotein: clinical significance and methods of analysis. *Crit Rev Clin Lab Sci* 1995;32:221-264.
8. Benchimol S, Ling V. P-glycoprotein and tumor progression. *J Natl Cancer Inst* 1994;86:814-816.
9. Rischin D, Ling V. Multidrug resistance in leukemia. In: Freireich EJ, Kantarjian H, eds. *Leukemia: advances in research and treatment*. Boston, Dordrecht, London: Kluwer Academic Publishers; 1993:269-293.
10. Goldstein LJ, Galski H, Fojo A, et al. Expression of a multidrug resistance gene in human cancers. *J Natl Cancer Inst* 1989;81:116-124.
11. Marie JP, Zittoun R, Sikic BI. Multidrug resistance (mdr1) gene expression in adult acute leukemias: correlations with treatment outcome and in vitro drug sensitivity. *Blood* 1991;78:586-592.
12. Piwnica-Worms D, Chiu ML, Budding M, Kronauge JF, Kramer RA, Croop JM. Functional imaging of multidrug-resistant Pgp with an organotechnetium complex. *Cancer Res* 1993;53:977-984.
13. Rao VV, Chiu ML, Kronauge JF, Piwnica-Worms D. Expression of recombinant human multidrug resistance p-glycoprotein in insect cells confers decreased accumulation of technetium-99m-sestamibi. *J Nucl Med* 1994;35:510-515.
14. Chiu ML, Kronauge JF, Piwnica-Worms D. Effect of mitochondrial and plasma membrane potentials on accumulation of hexakis (2-methoxyisobutylisonitrile) technetium(I) in cultured mouse fibroblasts. *J Nucl Med* 1990;31:1646-1653.
15. Piwnica-Worms D, Kronauge JF, Chiu ML. Uptake and retention of hexakis (2-methoxyisobutyl isonitrile) technetium(I) in cultured chick myocardial cells. Mitochondrial and plasma membrane potential dependence. *Circulation* 1990;82:1826-1838.
16. Duran Cordobes M, Starzes A, Delmon-Moingeon L, et al. Technetium-99m-uptake by human benign and malignant breast tumor cells: correlation with MDR gene expression. *J Nucl Med* 1996;37:286-289.

17. Kostakoglu L, Elahi N, Kiratli P, et al. Clinical validation of influence p-glycoprotein on the uptake of <sup>99m</sup>Tc-sestamibi in patients with malignant tumors. *J Nucl Med* 1997;38:1003-1008.
18. Kostakoglu L, Kiratli P, Ruacan S, et al. Association of tumor wash-out rates and accumulation of <sup>99m</sup>Tc-MIBI with the expression of p-glycoprotein in lung cancer. *J Nucl Med* 1998;39:228-234.
19. Del Vecchio S, Ciarmiello A, Potena MI, et al. In vivo detection of multi-drug resistant (MDR1) phenotype by technetium-99m-sestamibi scan in untreated breast cancer patients. *Eur J Nucl Med* 1997;24:150-159.
20. Chomczynski P and Sacchi N. Single step method for RNA isolation by acid guanidiniumthiocyanate-phenol chloroform extraction. *Ann Biochem* 1979;162:156-159.
21. Nussler V, Pelka Fleischer R, Zwierzina H, et al. Clinical importance of P-glycoprotein-related resistance in leukemia and myelodysplastic syndromes first experience with their reversal. *Ann Hematol* 1994;69:S25-29.
22. Kuwazuru Y, Yoshimura A, Hanada S, et al. Expression of the multidrug transporter p-glycoprotein in acute leukemia cells and correlation to clinical drug resistance. *Cancer* 1990;66:868-873.
23. Goasguen JE, Dossot J-M, Fardel O, et al. Expression of the multidrug resistance-associated p-glycoprotein (P-170) in 59 cases of de novo acute lymphoblastic leukemia: prognostic implications. *Blood* 1993;81:2394-2398.
24. Massart C, Gibassier J, Raoul M, et al. Cyclosporin A, verapamil and S9788 reverse doxorubicin resistance in a human medullary thyroid carcinoma cell line. *Anticancer Drugs* 1995;6:135-146.
25. Stewart AJ, Canitrot Y, Baracchini E, Dean NM, Deeley RG, Cole SP. Reduction of expression of the multidrug resistance protein (MRP) in human tumor cells by antisense phosphorothioate oligonucleotides. *Biochem Pharmacol* 1996;51:461-469.
26. Webb M, Raphael CL, Asbahr H, Erber WN, Meyer BF. The detection of rhodamine 123 efflux at low levels of drug resistance. *Br J Haematol* 1996;93:650-655.
27. Delville JP, Pradier O, Pauwels O, et al. Comparative study of multidrug resistance evaluated by means of the quantitative immunohistochemical detection of P-glycoprotein and the functional release of rhodamine 123. *Am J Hematol* 1995;49:183-193.
28. Bailly JD, Muller C, Jaffrezou JP, et al. Lack of correlation between expression and function of p-glycoprotein in acute myeloid leukemia cell lines. *Leukemia* 1995;9:799-807.
29. Jain RK. Transport of molecules in the tumor interstitium: a review. *Cancer Res* 1987;47:3039-3051.
30. Hanson CA. Immunophenotyping of hematologic malignant conditions: to flow or not to flow? *Ann J Clin Pathol* 1991;96:295-298.
31. Beck WT, Grogan TM, Willman CL, et al. Methods to detect p-glycoprotein-associated multidrug resistance in patients' tumors: consensus recommendations. *Cancer Res* 1996;56:3010-3020.
32. Meleforts O, Hentze MW. Translational regulation by mRNA/protein interactions in eucaryotic cells: ferritin and beyond. *Bioassays* 1993;15:85-90.
33. Rhoads RE. Regulation of eucaryotic protein synthesis by initiation factors. *J Biol Chem* 1993;268:3017-3020.

# Fluorine-18-Fluorouracil to Predict Therapy Response in Liver Metastases from Colorectal Carcinoma

Antonia Dimitrakopoulou-Strauss, Ludwig G. Strauss, Peter Schlag, Peter Hohenberger, Markus Möhler, Franz Oberdorfer and Gerhard van Kaick

*Department of Oncological Diagnostics and Therapy and Department of Radiochemistry and Radiopharmacology, German Cancer Research Center, Heidelberg; Department of Internal Medicine IV, University of Heidelberg, Heidelberg; and Department of Surgery and Surgical Oncology, Virchow-Klinikum, Robert-Rössle-Klinik, Berlin, Germany*

Prediction of chemotherapy response is still a problem in oncological patients. **Methods:** Studies with PET and <sup>18</sup>F-fluorouracil (FU) were used for measurements of drug concentrations in patients with liver metastases from colorectal carcinoma. The PET data obtained before onset of FU chemotherapy were correlated to the growth rate of the metastases after therapy. The final evaluation included 25 metastases obtained in 17 patients. CT preceded the first chemotherapeutic cycle and was repeated within 3-11 mo after onset of treatment. The uptake of the cytostatic agent was evaluated in the liver metastases using the SUV at 120 min after tracer infusion. Tumor growth rate of the metastases was calculated based on CT volumetric data. **Results:** The trapping of <sup>18</sup>F-FU was highly variable even for multiple metastases in the same patients. Six metastases with high <sup>18</sup>F-FU uptake values exceeding 3.0 SUV correlated with negative growth rate values, 5 of 25 metastases with intermediate uptake values ranging from 2.0-3.0 SUV were associated with almost stable growth rate values nearly zero and 14 of 25 metastases with low uptake values < 2.0 SUV demonstrated positive growth rate values. Only metastases with a <sup>18</sup>F-FU uptake exceeding 3.0 SUV at 120 min postinjection demonstrated a response to therapy. A significant correlation of 0.86 ( $p < 0.001$ ) was found between the <sup>18</sup>F-FU uptake values in the metastases measured before chemotherapy and the growth rate of the lesions after treatment. **Conclusion:** The data show, that FU chemotherapy outcome can be predicted using a single PET study with <sup>18</sup>F-FU before onset to therapy.

**Key Words:** PET; fluorine-18-fluorouracil; liver metastases; liver treatment

**J Nucl Med** 1998; 39:1197-1202

**M**etastatic disease to the liver remains a notable problem in the treatment of oncological patients. The median survival for patients with liver metastases from colorectal cancer is 4-12 mo from the time of diagnosis of metastatic disease. The response rate to chemotherapy is highly variable (1). The standard chemotherapeutic agent used in these patients is fluorouracil (FU), which is applied as a continuous infusion or concomitant with modulators. Another approach often used in patients with inoperable liver metastases is regional chemotherapy using a surgically implanted catheter in the gastroduodenal artery (2). However, the studies published in the literature are not conclusive with respect to the therapeutic outcome (3,4). This may depend on the patient populations examined by each author, since some investigators include only patients with liver-limited disease and other with extrahepatic disease. Another point is the different doses and schemes of the chemotherapeutic protocols and especially the different technique used for intra-arterial chemotherapy.

Furthermore, the comparison of the median survival time is variably documented among authors, varying from onset of diagnosis, onset of symptoms or initiation of treatment. Some authors use different criteria to evaluate response of liver metastases to therapy, including biochemical determinants such as liver enzymes or tumor-associated antigens such as carcino-

Received Jul. 8, 1997; revision accepted Oct. 13, 1997.  
For correspondence or reprints contact: Antonia Dimitrakopoulou-Strauss, MD, Department of Oncological Diagnostics and Therapy, German Cancer Research Center, Im Neuenheimer Feld 280, D-69120 Heidelberg, Germany.